

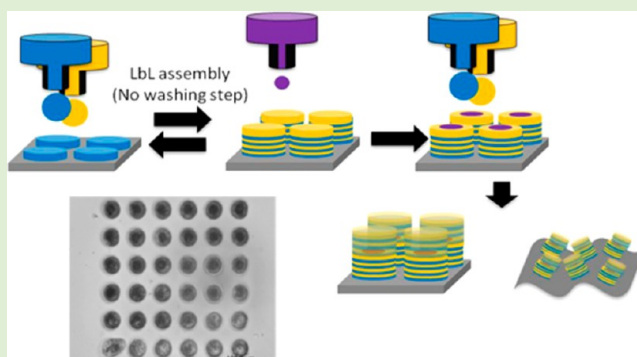
Inkjet Printing of Silk Nest Arrays for Cell Hosting

Rattanon Suntivich,[†] Irina Drachuk,[†] Rossella Calabrese,[‡] David L. Kaplan,[‡] and Vladimir V. Tsukruk*

[†]School of Materials Science and Engineering, Georgia Institute of Technology, Atlanta, Georgia 30332-0245, United States

[‡]Department of Biomedical Engineering, Tufts University, Medford, Massachusetts 02155, United States

ABSTRACT: An inkjet printing approach is presented for the facile fabrication of microscopic arrays of biocompatible silk “nests” capable of hosting live cells for prospective biosensors. The patterning of silk fibroin nests were constructed by the layer-by-layer (LbL) assembly of silk polyelectrolytes chemically modified with poly-(L-lysine) and poly-(L-glutamic acid) side chains. The inkjet-printed silk circular regions with a characteristic “nest” shape had diameters of 70–100 μm and a thickness several hundred nanometers were stabilized by ionic pairing and by the formation of the silk II crystalline secondary structure. These “locked-in” silk nests remained anchored to the substrate during incubation in cell growth media to provide a biotemplated platform for printing-in, immobilization, encapsulation and growth of cells. The process of inkjet-assisted printing is versatile and can be applied on any type of substrate, including rigid and flexible, with scalability and facile formation.



INTRODUCTION

Fabrication of large-scale functional arrays of organic, polymeric, or biological materials is a crucial challenge in the field of biosensing for the controlled placement of living cells on various substrates.¹ There are many advanced patterning techniques that can be utilized for the wet-fabrication of such arrays including inkjet printing, microcontact printing, micro-molding and dip-pen nanolithography.^{2–10} These techniques allow target molecules to be deposited on various substrates in controlled configurations with a variety of periodic patterns and the inclusion of components at different spatial scales. The selection of proper materials for such arrays, especially for environmentally sensitive cell-based biosensors, is a critical issue, where biocompatibility and natural material can offer significant benefits.

Among natural polymers considered for such applications, silk fibroin is one of the most promising materials due to its excellent physical, chemical, and biological properties.^{11–19} Silk has been used in medical sutures due to its biocompatibility. Silk can be applied as dispersant for hydrophobic materials due to its amphiphilic properties, and the protein in various material formats can be exploited as a tough matrix or as a universal binder for nanocomposite materials. The protein can be applied as flexible and optically transparent biomaterial for photonic devices, or used as a biocompatible scaffold for composite materials for biosensing applications.^{20–28} For biosensing, silk is a useful material because it can be genetically modified for production of specific silk properties.²⁹ Moreover, silk can be used for enzyme immobilization and stabilization for biosensing and for cell protection.^{30,31} The silk secondary structure can be changed from random coil (amorphous state) to β -sheet (crystalline state) structure upon controlled drying and with

methanol treatment.^{32,33} On the other hand, the solubility of silk can be improved by ionic polymer grafting such as with polylysine or polyglutamic acid.^{34,35}

Silk and modified silks are compatible with a variety of conventional wet-chemistry fabrication processes such as drop-casting, spin-casting, electrospinning, Langmuir–Blodgett deposition, and layer-by-layer (LbL) assembly. Among these, LbL technology is widely used to fabricate ultrathin coatings and complex materials from synthetic and natural polymers, nanoparticles, and fibers with a variety of functionalities, controlled thickness, permeability, strength, porosity, and environmentally responsive properties.^{36–50} In recent studies, responsive silk microcapsules have been assembled by electrostatic interactions.⁵¹ Combining biodegradable silk materials and LbL assembly was utilized for microcapsules and ultrathin coatings.^{52–54} In addition, the release properties could be tuned by changing treatment conditions.⁵⁵ However, making patterned arrays from silk materials with conventional micro-fabrication remains challenging due to long-term solution precipitation, need to work with low solution concentrations, and easily changing secondary structure.

Inkjet printing is a promising patterning process, widely applied to fabricate complex arrays on the microscopic level.^{56,57} In addition, this technique can be used to pattern target molecules such as protein on virtually any substrate, including those that are flexible, porous, and rigid, and the technique can be adapted to large scale manufacturing.⁵⁸ Inkjet printing is an outstanding candidate for bio patterning due to

Received: January 7, 2014

Revised: February 28, 2014

Published: March 7, 2014

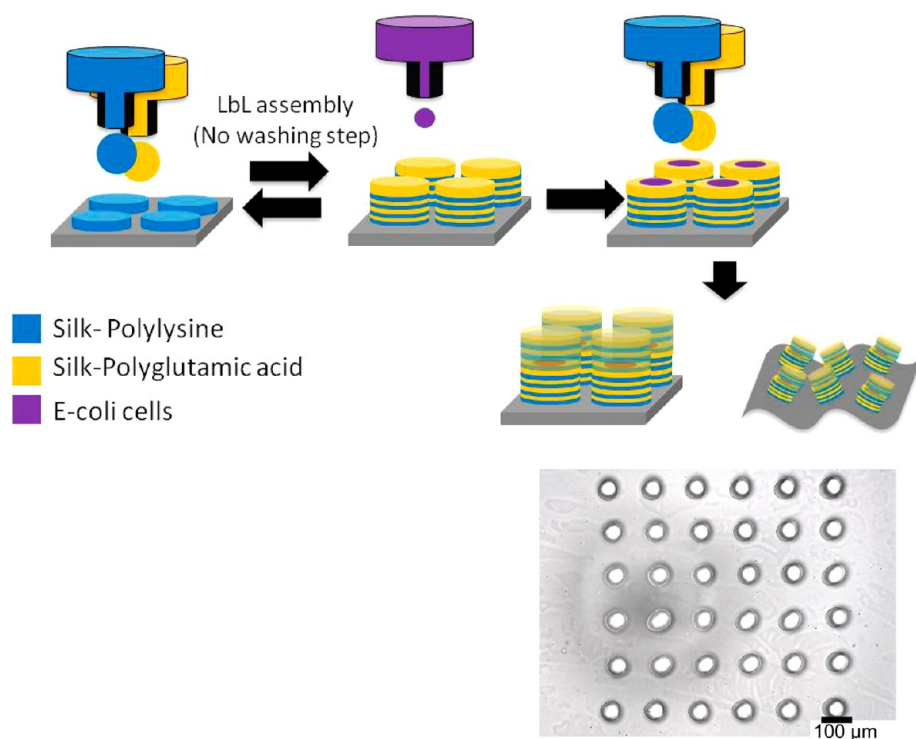


Figure 1. (Top) Fabrication process of inkjet-assisted silk array for cell encapsulation. (Bottom) Optical image of silk array with encapsulated cells.

mild patterning conditions, mark-less patterning and non-contact printing. The contact-free patterning prevents contamination from printing process that is crucial for biosensing applications.⁵⁹ Moreover, inkjet printing can be combined with LbL technology to fabricate patterns with controlled local thickness and from biological materials.^{60–63} However, robust inkjet printing of cell-based biosensors has not been demonstrated due to issues related to the damaging conditions of direct cell printing on solid supports.⁶⁴ Inkjet printing can be utilized for printing and coprinting of various biocompatible templates and living cells because of mild patterning processing conditions and potential scalability for fabrication of large (thousand dots) arrays of firmly tethered encapsulated bacterial cells which can potentially serve as multiplexing biosensors.⁶⁵ Furthermore, scaling down spatial dimensions of individual biotemplating dots to below 100 μm will allow for miniaturization of the resulting biosensing arrays.

Therefore, in this study, we focus on the facile fabrication of patterned arrayed substrates from biocompatible silk materials via inkjet printing technique. Successful patterning of silk arrays was constructed by the multiple LbL deposition of dots composed of ionomeric silk chemically modified with poly-(L-lysine) and poly-(L-glutamic acid) side chains. Robust inkjet-assisted circular LbL structures with diameters of $\sim 70\text{--}100\ \mu\text{m}$ were stabilized by ionic pairing and by the formation of silk II secondary structures to generate characteristic “nest” morphologies with well-defined rims on both rigid (glass) and flexible (polymer) substrates. These “locked-in” silk nests with depleted central regions and elevated rims remained anchored to the substrate during incubation in cell growth media, thereby providing a biocompatible platform for immobilization of biological cells without compromising their viability. Preliminary results show the ability for printing-in *E. coli* cells confined within these silk microscopic regions.

EXPERIMENTAL SECTION

Materials. Polystyrene (PS, $M_w = 250000$) and toluene (J.T. Baker grade) were purchased from VWR (San Dimas, CA). Anhydrous sodium carbonate (Na_2CO_3), lithium bromide (LiBr), sodium chloride (NaCl), and sodium monobasic phosphate (NaH_2PO_4) were purchased from Sigma-Aldrich (Saint Louis, MO). All chemicals were used without further modification. Nanopure water (Barnstead) with an 18.2 $\text{M}\Omega\text{-cm}$ resistivity was used for all experiments. Yeast extract, Bacto-trypton, casamino acids were purchased from BD Bioscience (San Jose, CA).

Silk was obtained from *Bombyx mori* silkworm cocoons as described previously.^{52,66} The solution was dialyzed with deionized water by using Slide-a-Lyzer dialysis cassettes (molecular weight cutoff (MWCO) 3500, Pierce) overnight at room temperature to remove the LiBr. Silk was modified to obtain cationic or anionic ionomers for electrostatic interaction by grafting polylysine ($M_w = 15\ \text{kDa}$) or polyglutamic acid ($M_w = 15\ \text{kDa}$) on silk molecules with diazonium activation of the abundant tyrosine side chains in the silk molecules followed by poly(amino acid) grafting, as we have described previously.^{51,67,68} *E. coli* (from Clontech Inc., Mountain View, CA) for printing were transformed to encode a theophylline synthetic riboswitch RS21.1.⁶⁹ For activation of riboswitch (RS), synthetic minimal medium (SMM) containing reduced concentration of amino acids was used along with theophylline stock solution (100 mM) in DMSO, which was diluted into assay to the final concentration of 5 mM. For printing, cells were collected in 15 mL centrifuge tubes by centrifugation at 3000 rpm for 2 min and washed three times with phosphate buffer (Na^+ 0.05 M and K^+ 0.1 M, pH 5.5) and kept in SMM medium.

Fabrication and Characterization. Inkjet patterns were fabricated by adjusting the pH of the silk-polylysine (1 mg/mL in 0.05 M NaH_2PO_4) to pH 5.5 and printing the silk solution on a PS-coated glass substrate to avoid silk film dewetting (Figure 1). A solution of silk-polyglutamic acid (1 mg/mL in 0.05 M NaH_2PO_4 , pH 5.5) was printed on top of silk-polylysine dots at the same positions to generate the first silk bilayer stabilized by ionic interactions. The printing process was repeated to produce the desired number of silk bilayers (number of bilayers from 1–10) without using washing during the intermediate steps (Figure 1). For preliminary evaluation of the

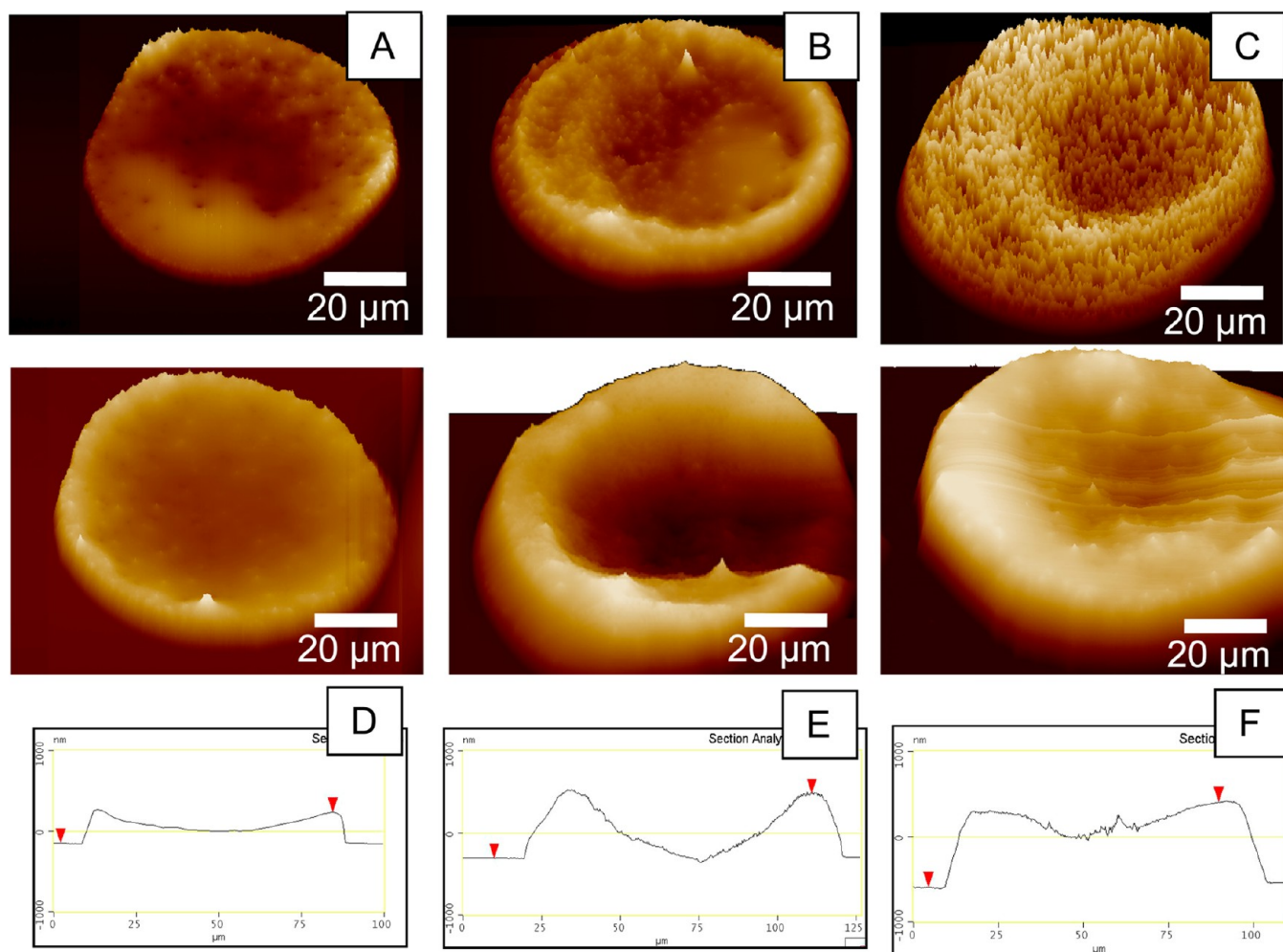


Figure 2. 3D surface morphology of silk nests inkjet-fabricated from 0.5 mg/mL (top) and 1 mg/mL (bottom) silk solutions at different numbers of silk bilayers: (A) 1 bilayer, (B) 3 bilayers, and (C) 5 bilayers. (D, E) Cross section of AFM images of 1 bilayer (D), 3 bilayers (E), and 5 bilayers (F) 1 mg/mL dot showing silk nest shape. The scan size is 100 μm for all images. Z-scale is 1000 nm for A–C and 2000 nm for D and E. Grooves and lines are caused by local damaging during scanning.

feasibility of silk arrays for cell encapsulation, the solution with *E. coli* was printed at the center of the silk nests, followed by capping the silk. A JetLab II inkjet printer (MicroFab Technologies) was used for experiments with a 50 μm nozzle diameter for all experiments in this study.

Surface morphology and thickness of inkjet-assisted ionomeric silk bilayers was characterized with atomic force microscopy (AFM). The AFM images were acquired by using a Dimension 3000 microscope in a “light” tapping mode according to our standard procedures.^{70,71} The silk arrays were gently dried and scanned at selected surface areas of 100 $\mu\text{m} \times 100 \mu\text{m}$, 20 $\mu\text{m} \times 20 \mu\text{m}$, and 5 $\mu\text{m} \times 5 \mu\text{m}$ using silicon cantilevers with a 330 kHz resonance frequency and 40 N/m spring constant. The silk dot thickness was measured at the center of the circular regions in the each array by using AFM cross-sectional analysis for multiple dots (five independent dots). Optical and fluorescence microscopy studies were performed on a DM 4000 M (Leica) microscope.

RESULTS AND DISCUSSION

Morphology of Silk Nest Arrays. The thickness of the deposited silk regions with diameters varying from 70 to 100 μm was controlled by varying the silk concentration and the number of printed silk bilayers. The shape and dot size of the array depended on the hydrophobicity and smoothness of the

substrate as well as deposition conditions (jet velocity, solution concentration) and overall alignment of the deposition steps.⁷²

The silk dot arrays were printed on hydrophobic substrates (glass coated with a thin PS film) to obtain uniform surface covering, to avoid severe dewetting during deposition and drying of aqueous solution, and to ensure a smaller dot size (below 100 μm). The freshly cleaned hydrophilic glass substrates resulted in fine dispersion of the solution and dewettable dot morphologies with larger sizes due to the spreading of the initial solution. The processing steps were similar to those described for the aqueous-based polymer arrays in our previous study.⁷³ The typical dot size for silk multilayered films was around 100 μm with minimal sizes reaching 70 μm .

Surface morphology of a typical silk structure prepared from 0.5 and 1 mg/mL silk solutions with 1, 3, and 5 bilayers is illustrated in Figure 2. The initial silk regions were uniform with thicker regions showing significant aggregation, a common behavior of silk materials on solid substrates at low solution concentrations due to a strong tendency for silk molecules to form nanofibrillar bundles and globular aggregates with strong intermolecular interactions.^{74–77} Increasing silk solution concentration and the number of deposition cycles (number

of bilayers) resulted in more uniform, round silk regions (Figures 2 and 3). All dot-like deposited silk regions with

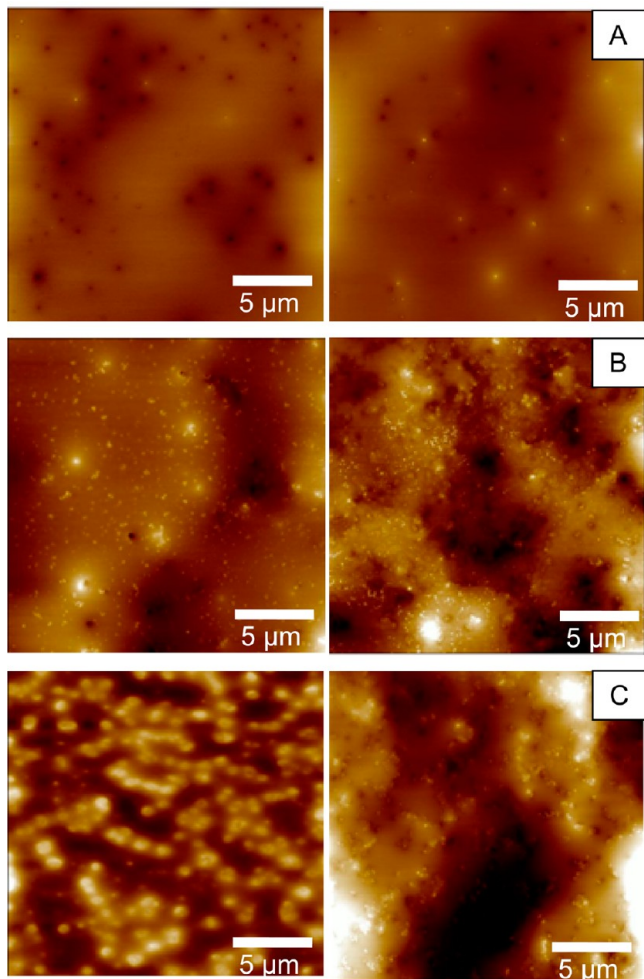


Figure 3. Surface morphology of 0.5 mg/mL (left) and 1 mg/mL (right) inkjet-assisted silk-polylysine/silk-polyglutamic acid at different number of bilayer: (A) 1 BL, (B) 3 BL, and (C) 5 BL. Z-scale is 1000 nm for all images.

different numbers of silk bilayers possessed characteristic “nest” shapes. The cross-section (Figure 2D–E) of these regions showed elevated rims (430 nm height for 1 bilayer regions) and depleted central regions (150 nm; Figure 2D).

Such a characteristic shape is caused by a complex balance of solution impact, outward microflow distribution, and different evaporation rates between the center and the periphery of the deposited material during formation of so-called coffee-ring structures.^{78–80} Overall, a capillary-driven outward flow from the center of the silk dots to the edge resulted in the excessive accumulation of material and higher silk thickness at the edge of round regions.⁸¹ Occasional misprints caused by various instrumental factors (e.g., step-motor missteps or microdroplet deviations) might lead to individual “defective” shape compromises for less than 5% of dots of larger arrays.

Such “nest” shapes have been observed in our previous studies of inkjet printing of LbL arrays from synthetic polyelectrolytes but are more pronounced here, probably due to the higher viscosity of the silk solution used in the present experiments.⁷³ The overall morphology of the silk dots can be controlled by adjusting the evaporation rate, solution

concentration, and drying temperature.^{82–84} The microroughness of silk regions (measured within $10\ \mu\text{m} \times 10\ \mu\text{m}$ surface areas) decreased significantly with increasing solution concentration and higher thickness of the silk regions: from 6.1 to 4.6 nm for the thinnest deposits and from 58.7 to 9.1 nm to the thicker (5 bilayers) silk dots (Figure 3).

The thickness of these silk nests, as measured from cross-section profiles in the central region, increased from 100 to 600 nm, with an increasing number of bilayers from 1 to 5 and with increasing solution concentration (Figure 4). The growth

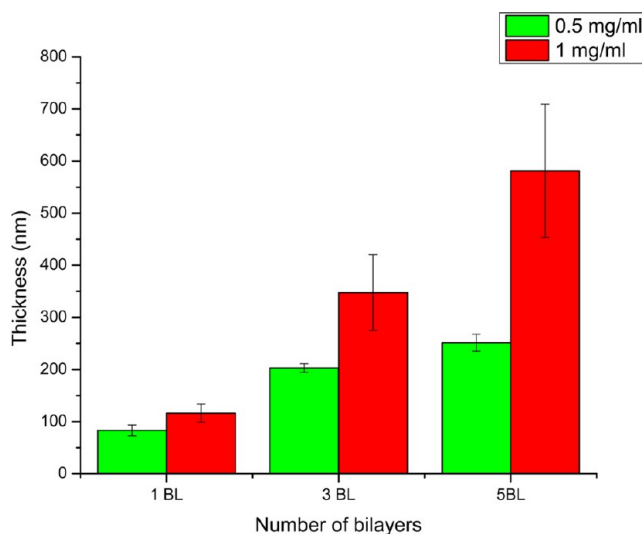


Figure 4. Thickness at the center of silk nests fabricated from 0.5 mg/mL and 1 mg/mL silk solutions with different numbers of bilayers.

characteristics of the silk regions during inkjet deposition of ionic silks were similar to conventional LbL films, with a linear regime controlled by ion pair interactions.⁸⁵ However, the average thickness of 115 nm per bilayer was much higher than the average thickness of other LbL films prepared from synthetic and natural polyelectrolytes fabricated by traditional dip- and spin-assisted LbL methods (around 4–6 nm per bilayer).^{86,87} This high average thickness per bilayer may be attributed to the partial transition of silk molecules from silk I (water-soluble) to silk II (water insoluble) form during shear stress, which locks in the silk materials in water insoluble forms.^{88,89} The partial transformation of the silk molecule from shear stress can be generated by high pressure inside inkjet nozzles and impact of the silk droplets on the substrates. In addition, the absence of washing intermediate steps caused remaining excessive ionic silk molecules, which increased overall thickness of the silk nest.

It is important to note that the elimination of washing steps between depositions due to the continuous inkjet deposition process is, in part, responsible for excessive accumulation of silk material, in contrast to traditional LbL technology with intermediate washing steps. This excessive material does not decrease the global stability of the nest morphologies due to the subsequent conversion to stable silk II format. In contrast, it is important to note that very small microdroplet volumes (60–90 pL) of silk solution used to fabricate the silk nests in a single deposition step limits the overall amount of silk material delivered in a single spot and allows for consistent growth of the silk dots without clogging the silk dot arrays. Finally, some

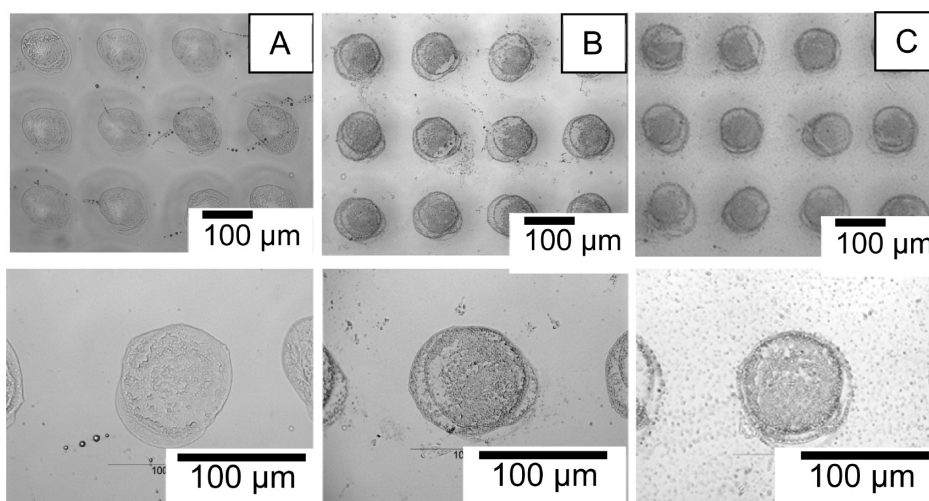


Figure 5. Optical images at different magnifications of inkjet-assisted silk nests (3 bilayers) at different exposure times in SMM media (A) before exposure, (B) after exposure for 30 min, and (C) after exposure overnight. Occasional misplacement of deposited dots can be clearly observed here.

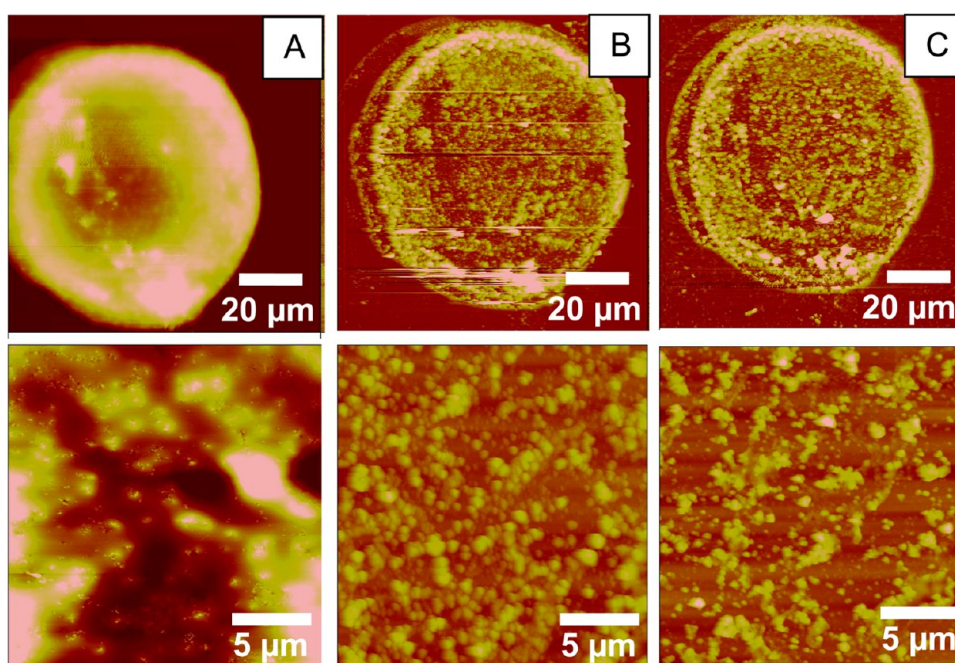


Figure 6. AFM images at different magnifications of inkjet-assisted silk nests (3 bilayers) at different exposure times in SMM media (A) before exposure, (B) after exposure for 30 min, and (C) after exposure overnight. Z-scale is 1000 nm for all images.

excessive silk material could be partially removed by exposing the silk nests to aggressive cell media as discussed below.

Stability of Inkjet Array of Silk Nests. In order to test the stability of silk nest arrays in liquid media for further encapsulation of cells, the arrays were exposed in a SMM medium for different periods of times (Figure 5). The general shape of the silk nest arrays remained intact after exposure to the cell media for 12 h. However, the excessive silk material was partially removed during the immersion in SMM media based on the AFM images of silk dots collected at different magnifications (Figure 6). Such removal resulted in a significant reduction of silk dot thickness (from approximately 400 to 150 nm) immediately after exposure to cell media (Figure 7). This removal of silk material stabilizes at longer exposure times (2–12 h) with some possible rearrangement of silk protein molecules of material or more likely swelling of the silk.^{90,91}

The inkjet printing process can be applied to various targeted substrates with proper wetting properties with respect to the aqueous silk solution. A substrate should be partial wetting by aqueous solution and can be instantly dried without significant swelling. The fabrication process can be applicable to modestly hydrophobic substrates, both rigid and flexible. One of those arrays is demonstrated for commercial PET plastic film in Figure 8.

Applicability of Inkjet Silk Nest Arrays for Cell Encapsulation. For preliminary studies of the applicability of these silk nest arrays for cell encapsulation, *E. coli* was inkjet printed in 6×6 arrays directly on preprinted silk arrays according to the fabrication process (Figure 1). *E. coli* dispersions in cell media were injected in the center of the dried silk nest regions and additional silk bilayers were

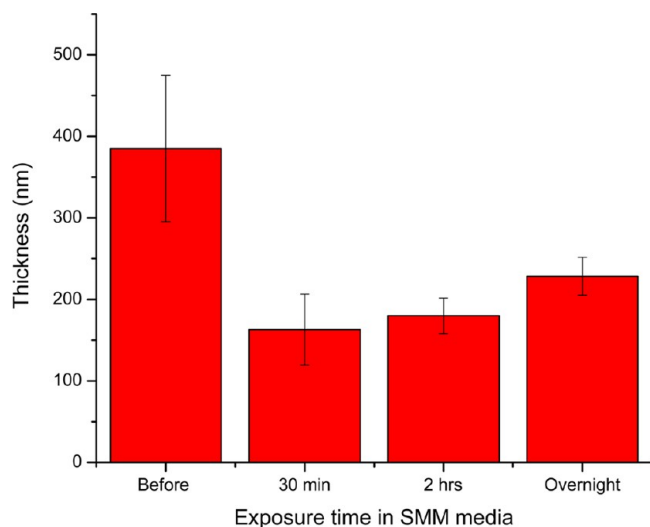


Figure 7. Thickness at the center of inkjet-assisted silk nests (1 mg/mL, 3 bilayers) after different exposure times in SMM media.

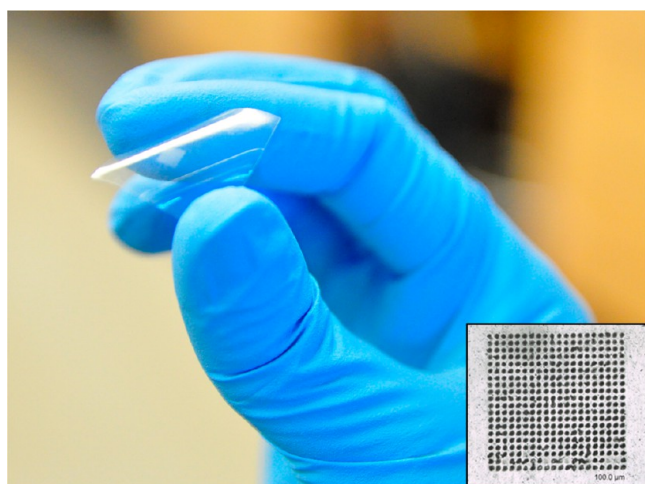


Figure 8. Inkjet array (20 × 20) of silk nests on a flexible PET substrate. Inset is a high resolution optical image of this array.

deposited on top of the *E. coli* cells to complete the encapsulation process.

The optical microscopy demonstrated that the inkjet printed *E. coli* cells could be consistently encapsulated within the silk dots (Figure 9). Encapsulated cell spreading was limited to the circular silk nest regions and the injected cells were confined

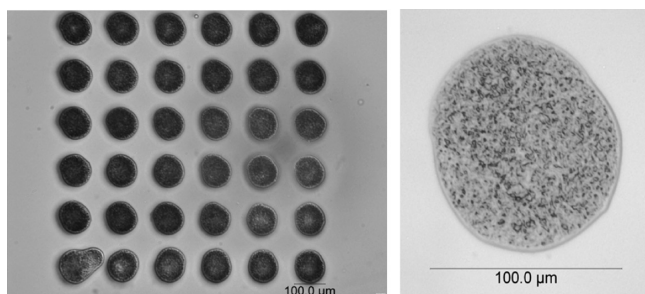


Figure 9. Optical images of silk nest arrays with imprinted *E. coli* cells (darker microscopic dots within silk region) strictly confined by the silk rim.

within the rim of silk regions, which serve as a natural barrier to cell spreading across the whole substrate (see high resolution optical image in Figure 9). Furthermore, the AFM images confirmed the high density of cell encapsulation within the individual circular silk regions and the preservation of their characteristic cylindrical shapes after the impact and forced jet-assisted deposition on the silk-pretreated nest-shape regions of arrays (Figure 10).

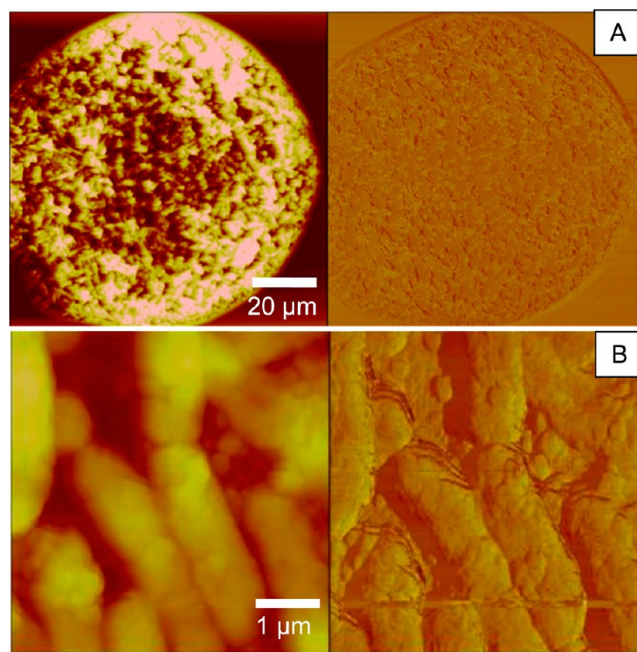


Figure 10. Surface morphology (left) and phase (right) of silk nests with encapsulated *E. coli* cells (3 silk bilayers-cell-3 silk bilayers). A) Low resolution and B) high resolution AFM image. Z-scale is 1500 nm for all topographical images.

CONCLUSIONS

An inkjet printing approach was demonstrated for the formation of microscopic arrays of silk nests capable of hosting cells for prospective biosensing applications. The successful patterning of silk fibroin LbL multilayer regions constructed from ionomeric silk materials with anionic and cationic side chains was demonstrated. The inkjet-assisted LbL multilayer structures, with up to 400 silk dots explored in this study, with diameters of about 100 μm and average thickness of 100–600 nm possessed characteristic nest shapes with depleted central regions and elevated rims. These silk-rich regions were formed during inkjet printing as a result of solution outflow after impact and are stabilized by ionic pairing followed by the formation of insoluble silk II as a result of drying. These “locked-in” silk nests remained anchored to the substrate during incubation in cell media providing a biocompatible, organized, platform for printing-in and the encapsulation of *E. coli* cells without compromising cell shape or function.

We suggest that the process of inkjet assisted printing of natural silk material is robust and versatile and can be applied on any type of modestly hydrophobic and robust substrate, both rigid and flexible, as demonstrated here for hydrophobized glass and flexible PET. It is worth noting that inkjet printing technology can be readily scalable for the fabrication of larger arrays, beyond 20 × 20 arrays fabricated here. This may require

additional efforts to avoid clogging of nozzles and increased stability of cell dispersions. This approach has intriguing potential for the facile formation of multiplexed arrays from biocompatible materials and for the immobilization of different cells for further exploration as multiplexing biosensing microarrays for biodetection of multiple chemical and biological species. The overall of silk multi deposition using inkjet printing was uniform with only occasional defects, and consistent patterning for future biosensing application. Overall, this fabrication process shows potential for the universal and large scale fabrication of biocompatible dot array templates with practical processing times on various practical substrates. Indeed, preliminary results showed successful printing-in of *E. coli* cells into these silk dots without compromising their integrity as will be discussed in detail elsewhere.

AUTHOR INFORMATION

Corresponding Author

*E-mail: vladimir@mse.gatech.edu.

Notes

The authors declare no competing financial interest.

ACKNOWLEDGMENTS

Funding from the FA9550-10-1-0172 and FA9550-09-1-0162 (BIONIC Center) Projects from Air Force Office of Scientific Research and SCG Paper PLC (Fellowship for R.S.) are gratefully acknowledged. The authors thank Dr. S. Harbaugh and Dr. N. Kelley-Loughnane (AFRL at Wright Patterson AFB, Dayton, OH) for providing the *E. coli* cells, Dr. Ikjun Choi, Kesong Hu, and Dr. Dhaval Kulkarni (Georgia Institute of Technology, Atlanta, GA) for technical assistance.

REFERENCES

- (1) Morgan, H.; Pritchard, D. J.; Cooper, J. M. *Biosens. Bioelectron.* **1995**, *10*, 841–846.
- (2) deGans, B. J.; Duineveld, P. C.; Schubert, U. S. *Adv. Mater.* **2004**, *16*, 203–213.
- (3) Singh, M.; Haverinen, H. M.; Dhagat, P.; Jabbour, G. E. *Adv. Mater.* **2010**, *22*, 673–685.
- (4) Gates, B. D.; Xu, Q.; Stewart, M.; Ryan, D.; Willson, C. G.; Whitesides, G. M. *Chem. Rev.* **2005**, *105*, 1171–1196.
- (5) Whitesides, G. M.; Ostuni, E.; Takayama, S.; Jiang, X.; Ingber, D. E. *Annu. Rev. Biomed. Eng.* **2001**, *3*, 335–373.
- (6) Xia, Y.; Whitesides, G. M. *Angew. Chem., Int. Ed.* **1998**, *37*, 550–575.
- (7) Jiang, X.; Zheng, H.; Gourdin, S.; Hammond, P. T. *Langmuir* **2002**, *18*, 2607–2615.
- (8) Quist, A. P.; Pavlovic, E.; Oscarsson, S. *Anal. Bioanal. Chem.* **2005**, *381*, 591–600.
- (9) Hecke, M.; Schomburg, W. K. *J. Micromech. Microeng.* **2004**, *14*, R1–R14.
- (10) Piner, R. D.; Zhu, J.; Xu, F.; Hong, S.; Mirkin, C. A. *Science* **1999**, *28*, 661–663.
- (11) Dornelles Mello, L. D.; Kubota, L. T. *Food Chem.* **2002**, *77*, 237–256.
- (12) Jiang, C.; Wang, X.; Gunawidjaja, R.; Lin, Y.-H.; Gupta, M. K.; Kaplan, D. L.; Naik, R. R.; Tsukruk, V. V. *Adv. Funct. Mater.* **2007**, *17*, 2229–2237.
- (13) Shao, Z.; Vollrath, F. *Nature* **2002**, *418*, 741.
- (14) Jin, H.-J.; Kaplan, D. L. *Nature* **2003**, *424*, 1057–1061.
- (15) Vollrath, F.; Madsen, B.; Shao, Z. *Proc. R. Soc. London, Ser. B* **2001**, *268*, 2339–2346.
- (16) Chen, X.; Shao, Z.; Vollrath, F. *Soft Matter* **2006**, *2*, 448–451.
- (17) Hu, K.; Gupta, M. K.; Kulkarni, D. D.; Tsukruk, V. V. *Adv. Mater.* **2013**, *25*, 2301–2307.
- (18) Gupta, M. K.; Singamaneni, S.; McConney, M.; Drummy, L. F.; Naik, R. R.; Tsukruk, V. V. *Adv. Mater.* **2010**, *22*, 115–119.
- (19) Kharlampieva, E.; Zimmitsky, D.; Gupta, M.; Bergman, K. N.; Kaplan, D. L.; Naik, R. R.; Tsukruk, V. V. *Chem. Mater.* **2009**, *21*, 2696–2704.
- (20) Kim, H.-S.; Yoon, S. H.; Kwon, S.-M.; Jin, H.-J. *Biomacromolecules* **2009**, *10*, 82–86.
- (21) Wang, S.; Zhang, Y.; Wang, H.; Yin, G.; Dong, Z. *Biomacromolecules* **2009**, *10*, 2240–2244.
- (22) Yina, H.; Aia, S.; Shia, W.; Zhu, L. *Sens. Actuators B* **2009**, *137*, 747–753.
- (23) Amsden, J. J.; Domachuk, P.; Gopinath, A.; White, R. D.; Negro, L. D.; Kaplan, D. L.; Omenetto, F. G. *Adv. Mater.* **2010**, *22*, 1–4.
- (24) Hu, K.; Tolentino, L. S.; Kulkarni, D. D.; Ye, C.; Kumar, S.; Tsukruk, V. V. *Angew. Chem., Int. Ed.* **2013**, *52*, 13784–13788.
- (25) Kharlampieva, E.; Kozlovskaya, V.; Wallet, B.; Shevchenko, V. V.; Naik, R. R.; Vaia, R.; Kaplan, D. L.; Tsukruk, V. V. *ACS Nano* **2010**, *4*, 7053–7063.
- (26) Young, S. L.; Gupta, M.; Hanske, C.; Fery, A.; Scheibel, T.; Tsukruk, V. V. *Biomacromolecules* **2012**, *13*, 3189–3199.
- (27) Krishnaji, S. T.; Huang, W.; Rabotyagova, O.; Kharlampieva, E.; Choi, I.; Tsukruk, V. V.; Naik, R.; Cebe, P.; Kaplan, D. L. *Langmuir* **2011**, *27*, 1000–1008.
- (28) Kharlampieva, E.; Kozlovskaya, V.; Gunawidjaja, R.; Shevchenko, V. V.; Vaia, R.; Naik, R. R.; Kaplan, D. L.; Tsukruk, V. V. *Adv. Funct. Mater.* **2010**, *20*, 840–846.
- (29) Mori, H.; Tsukadar, M. *Rev. Mol. Biotechnol.* **2000**, *74*, 95–103.
- (30) Zhanga, Y.-Q.; Shena, W.-D.; Gub, R.-A.; Zhuc, J.; Xue, R.-Y. *Anal. Chim. Acta* **1998**, *369*, 123–128.
- (31) Drachuk, I.; Shchepelina, O.; Harbaugh, S.; Kelley-Loughnane, N.; Stone, M.; Tsukruk, V. V. *Small* **2013**, *9*, 3128–3137.
- (32) Tsukada, M.; Gotoh, Y.; Nagura, M.; Minoura, N.; Kasai, N.; Freddi, G. *J. Polym. Sci., Part B: Polym. Phys.* **1994**, *32*, 961–968.
- (33) Hu, X.; Kaplan, D.; Cebe, P. *Macromolecules* **2006**, *39*, 6161–6170.
- (34) Numata, K.; Subramanian, B.; Currie, H. A.; Kaplan, D. L. *Biomaterials* **2009**, *30*, 5775–5784.
- (35) Nagano, A.; Kikuchi, Y.; Sato, H.; Nakazawa, Y.; Asakura, T. *Macromolecules* **2009**, *42*, 8950–8958.
- (36) Lvov, Y.; Möhwal, H. *Protein Architecture: Interfacial Molecular Assembly and Immobilization Biotechnology*; Marcel Dekker: New York, 2000; pp 1–394.
- (37) Hammond, P. T. *Adv. Mater.* **2004**, *16*, 1271–1293.
- (38) Stuart, M. C.; Huck, W.; Genzer, J.; Müller, M.; Ober, C.; Stamm, M.; Sukhorukov, G.; Szleifer, I.; Tsukruk, V. V.; Urban, M.; Winnik, F.; Zauscher, S.; Luzinov, I.; Minko, S. *Nat. Mater.* **2010**, *9*, 101–113.
- (39) Ko, H.; Jiang, C.; Tsukruk, V. V. *Chem. Mater.* **2005**, *17*, 5489–5497.
- (40) Zhao, W.; Xu, J.-J.; Shi, C.-G.; Chen, H.-Y. *Langmuir* **2005**, *21*, 9630–9634.
- (41) Kotov, N. A.; Dékány, I.; Fendler, J. H. *Adv. Mater.* **1996**, *8*, 637–641.
- (42) Zheng, H.; Lee, I.; Rubner, M. F.; Hammond, P. T. *Adv. Mater.* **2002**, *14*, 569–572.
- (43) Kinnane, C. R.; Such, G. K.; Caruso, F. *Macromolecules* **2011**, *44*, 1194–1202.
- (44) Sukhishvili, S. A. *Curr. Opin. Colloid Interface Sci.* **2005**, *10*, 37–44.
- (45) Zhang, H.; Fu, Y.; Wang, D.; Wang, L.; Wang, Z.; Zhang, X. *Langmuir* **2003**, *19*, 8497–8502.
- (46) Ariga, K.; Ji, Q.; Hill, J. P. *Adv. Polym. Sci.* **2010**, *229*, 51–87.
- (47) Choi, J.; Rubner, M. F. *Macromolecules* **2005**, *38*, 116–124.
- (48) Jiang, C.; Tsukruk, V. V. *Adv. Mater.* **2006**, *18*, 829–840.
- (49) Lost, R. M.; Crespilho, F. N. *Biosens. Bioelectron.* **2012**, *31*, 1–10.
- (50) Caruso, F.; Susha, A. S.; Giersig, M.; Mohwald, H. *Adv. Mater.* **1999**, *11*, 950–953.

- (51) Ye, C.; Shchepelina, O.; Calabrese, R.; Drachuk, I.; Kaplan, D. L.; Tsukruk, V. V. *Biomacromolecules* **2011**, *12*, 4319–4325.
- (52) Shchepelina, O.; Drachuk, I.; Gupta, M. K.; Lin, J.; Tsukruk, V. V. *Adv. Mater.* **2011**, *23*, 4655–4660.
- (53) Ye, C.; Drachuk, I.; Calabrese, R.; Dai, H.; Kaplan, D. L.; Tsukruk, V. V. *Langmuir* **2012**, *28*, 12235–12244.
- (54) Wallet, B.; Kharlampieva, E.; Campbell-Proszowska, K.; Kozlovskaya, V.; Malak, S.; Ankner, J. F.; Kaplan, D. L.; Tsukruk, V. V. *Langmuir* **2012**, *28*, 11481–11489.
- (55) Wang, X.; Hu, X.; Daley, A.; Rabotyagova, O.; Peggy, C. P.; Kaplan, D. L. *J. Controlled Release* **2007**, *121*, 190–199.
- (56) Calvert, P. *Chem. Mater.* **2001**, *13*, 3299–3305.
- (57) Tekin, E.; Smith, P. J.; Schubert, U. S. *Soft Matter* **2008**, *4*, 703–713.
- (58) Fujie, T.; Desii, A.; Ventrelli, L.; Mazzolai, B.; Mattoli, V. *Biomed. Microdev.* **2012**, *14*, 1069–1076.
- (59) Delaney, J. T.; Smith, P. J.; Schubert, U. S. *Soft Matter* **2009**, *5*, 4866–4877.
- (60) Yang, S. Y.; Rubner, M. F. *J. Am. Chem. Soc.* **2002**, *124*, 2100–2101.
- (61) Settia, L.; Fraleoni, M. A.; Ballarinb, B.; Filippinia, A.; Frascaroa, D.; Piana, C. *Biosens. Bioelectron.* **2005**, *20*, 2019–2026.
- (62) L. Settia, L.; Fraleoni-Morgera, A.; Mencarellia, I.; Filippini, A.; Ballarinb, B.; Biase, M. D. *Sens. Actuators B* **2007**, *126*, 252–257.
- (63) Bernacka-Wojcik, I.; Senadeera, R.; Wojcik, P. J.; Silva, L. B.; Doria, G.; Baptista, P.; Aguas, H.; Fortunato, E.; Martins, R. *Biosens. Bioelectron.* **2010**, *25*, 1229–1234.
- (64) Ringeisen, B. R.; Pirlo, R. K.; Wu, P. K.; Boland, T.; Huang, Y.; Sun, W.; Hamid, Q.; Chrisey, D. B. *MRS Bull.* **2013**, *38*, 834–843.
- (65) Davidson, M. E.; Harbaugh, S. V.; Chushak, Y. G.; Stone, M. O.; Kelley-Loughnane, N. *ACS Chem. Biol.* **2013**, *8*, 234.
- (66) Phillips, D. M.; Drummy, L. F.; Conrady, D. G.; Fox, D. M.; Naik, R. R.; Stone, M. O.; Trulove, P. C.; Long, H. C. D.; Mantz, R. A. *J. Am. Chem. Soc.* **2004**, *126*, 14350–14351.
- (67) Serban, M. A.; Kaplan, D. L. *Biomacromolecules* **2010**, *11*, 3406–3412.
- (68) Calabrese, R.; Kaplan, D. L. *Biomaterials* **2012**, *33*, 7375–7385.
- (69) Harbaugh, S.; Kelley-Loughnane, N.; Davidson, M.; Narayanan, L.; Trott, S.; Chushak, Y. G.; Stone, M. O. *Biomacromolecules* **2009**, *32*, 1610–1614.
- (70) Tsukruk, V. V.; Reneker, D. H. *Polymer* **1995**, *36*, 1791–1808.
- (71) McConney, M. E.; Singamaneni, S.; Tsukruk, V. V. *Polym. Rev.* **2010**, *50*, 235–286.
- (72) Wang, J. Z.; Zheng, Z. H.; Li, H. W.; Huck, W. T. S.; Siringhaus, H. *Nat. Mater.* **2004**, *3*, 171–176.
- (73) Suntivich, R.; Shchepelina, O.; Choi, I.; Tsukruk, V. V. *ACS Appl. Mater. Interfaces* **2012**, *4*, 3102–3110.
- (74) Reiter, G. *Langmuir* **1993**, *9*, 1344–1351.
- (75) Reiter, G. *Phys. Rev. Lett.* **1992**, *68*, 75–78.
- (76) Shulha, H.; Wong, C.; Kaplan, D. D.; Tsukruk, V. V. *Polymer* **2006**, *47*, 5821–5830.
- (77) Wallet, B.; Kharlampieva, E.; Campbell-Proszowska, K.; Kozlovskaya, V.; Malak, S.; Ankner, J. F.; Kaplan, D. L.; Tsukruk, V. V. *Langmuir* **2012**, *28*, 13345–13353.
- (78) Shen, X.; Ho, C.-M.; Wong, T.-S. *J. Phys. Chem. B* **2010**, *114*, 5269–5274.
- (79) Weon, B. M.; Je, J. H. *Phys. Rev. E* **2010**, *82*, 015305–4.
- (80) Hong, S. W.; Jeong, W.; Ko, H.; Kessler, M. R.; Tsukruk, V. V.; Lin, Z. *Adv. Funct. Mater.* **2008**, *18*, 2114–2122.
- (81) Sharma, V.; Park, K.; Srinivasarao, M. *Mater. Sci. Eng., R* **2009**, *65*, 1–38.
- (82) Deegan, R. D.; Bakajin, O.; Dupont, T. F.; Huber, G.; Nagel, S. R.; Witten, T. A. *Nature* **1997**, *389*, 827–829.
- (83) Xu, J.; Xia, J.; Hong, S. W.; Lin, Z.; Qiu, F.; Yang, Y. *Phys. Rev. Lett.* **2006**, *96*, 066104–066108.
- (84) Soltman, D.; Subramanian, V. *Langmuir* **2008**, *24*, 2224–2231.
- (85) Choi, I.; Suntivich, R.; Plamper, F. A.; Synsachke, C. V.; Müller, A. H. E.; Tsukruk, V. V. *J. Am. Chem. Soc.* **2011**, *133*, 9592–9606.
- (86) Zhuk, A.; Pavlukhina, S.; Sukhishvili, S. A. *Langmuir* **2009**, *25*, 14025–14029.
- (87) Kozlovskaya, V. A.; Kharlampieva, E. P.; Erel-Unal, I.; Sukhishvili, S. A. *Polym. Sci., Ser. A* **2009**, *51*, 719–729.
- (88) Knight, D. P.; Knight, M. M.; Vollrath, F. *Int. J. Biol. Macromol.* **2000**, *27*, 205–210.
- (89) Ha, S.-W.; Tonelli, A. E.; Hudson, S. M. *Biomacromolecules* **2005**, *6*, 1722–1731.
- (90) Jin, H.-J.; Park, J.; Karageorgiou, V.; Kim, U.-J.; Valluzzi, R.; Cebe, P.; Kaplan, D. L. *Adv. Funct. Mater.* **2005**, *15*, 1241–1247.
- (91) Lawrence, B. D.; Wharram, S.; Kluge, J. A.; Leisk, G. G.; Omenetto, F. G.; Rosenblatt, M. I.; Kaplan, D. L. *Macromol. Biosci.* **2010**, *10*, 393–403.